Electron-Impact Spectroscopy *

By Aron Kuppermann † and L. M. Raff ‡

Noyes Chemical Laboratory, University of Illinois, Urbana, Ill., U.S.A.

Received 29th January, 1963

A spectrometer has been devised for determining electronic energy levels of molecules by inelastic scattering of low-energy electrons. It permits the detection of optically forbidden electronic transitions as clearly as optically allowed ones in a routine manner. The spectrometer has been used to obtain excitation spectra for helium, argon, hydrogen and ethylene. For the first three of these substances, the spectra agree with previous experiments. For ethylene, in addition to optically allowed transitions, two forbidden ones occur at about 4·6 and 6·5 eV. Variation of peak heights with incident electron beam energy suggest that the first corresponds to a triplet state but that the second does not.

Franck and Hertz [1] used the measurement of energy losses of electron swarms in atomic gases as a means of determining the lowest excitation energies of those gases. However, such electron-impact techniques have not been used to any appreciable extent for the determination of electronic energy levels of molecules. The reasons are: first, because electrons can produce rotational and vibrational excitation of the ground electronic states of molecules, it is not possible to use experimental techniques in which the electrons build up energy slowly between collisions if one wishes to determine the electronic levels of those molecules. Therefore, one must use single-scattering electron beam techniques, which require more elaborate set-ups. Secondly, because of the relatively simple optical techniques which permit great accuracy in the determination of photon energies, optical spectroscopy provides a simpler method of much higher resolution for the measurement of electronic transitions in atoms and molecules.

The development of metal high vacuum techniques and of electronic circuitry have simplified the construction and operation of single-scattering electron-impact spectrometers. In addition, there exists an extremely powerful reason for using low-energy electron impact as a spectroscopic tool. This is the difference in the selection rules for excitation of electronic energy levels of atoms and molecules by photons and by electrons. Practically all electronic transitions are allowed when low-energy electrons are used.[2] They include transitions which are spin-forbidden and/or symmetry-forbidden when photons are used. Therefore, low-energy electron-impact spectroscopy provides in principle a technique which permits determination of such optically forbidden electronic transitions, as well as optically allowed ones. In addition, transition energies above 11 eV, which are difficult to deal with optically, can be easily studied with electron-impact techniques.

The inelastic scattering of low-energy electrons by molecules has been experimentally studied by a number of researchers. The molecules studied include hydrogen,[3] oxygen,[4] nitrogen,[5] carbon monoxide [6] and carbon dioxide.[6] However, most studies were directed either to the measurement of scattering cross-sections or to the determination of the appearance potentials of assorted ions. Studies aimed mainly at the determination of electronic energy levels in molecules were relatively scarce.

* Supported in part by funds from the U.S. Atomic Energy Commission.

† present address: Gates and Crellin Lab. of Chem., California Inst. of Technology, Pasadena.

‡ present address: Dept. of Chem., Columbia University, New York.

There have been two important recent studies; first, Lassettre and his students [7] have constructed an electron-impact spectrometer with which they have made accurate measurements of differential scattering cross-sections in several atoms and molecules. However, they have worked mainly with electrons whose incident energy was between 400 and 600 eV. In this region the Born approximation [8] is valid, and transitions involving change of spin multiplicity are forbidden. Therefore, in those experiments Lassettre does not see such transitions. However, in measurements made with incident energies below 100 eV, forbidden transitions were observed.[7] Secondly, Schulz [9] has used a low-energy electron impact method for determining electronic transitions in H_2 and H_2O. The energy of the incident beam is scanned, and the electrons which lose all but a small energy (usually about 0·3 eV) are trapped in a potential well and detected. This method, which also permits the observation of optically forbidden transitions, is further discussed later.

In this paper we describe the use of a low-energy electron-impact spectrometer in which optically forbidden electronic transitions in molecules can usually be detected as clearly and easily as optically allowed ones.[10] Spectra for He, Ar, H_2 and C_2H_4 are given and discussed.

DESIGN AND CONSTRUCTION OF APPARATUS

The design and construction of the spectrometer is based in part on the apparatus used by Arnot and Baines [11] to measure collision cross-sections of electrons with mercury atoms. Our version consists essentially of two differentially pumped high-vacuum chambers, an electron gun chamber, and a collision chamber, connected through a 1·5 mm diam. pinhole. A beam of approximately mono-energetic electrons is produced in the gun chamber and enters the collision chamber through that pinhole. There the electrons undergo collisions with the molecules being studied, and the energy losses of electrons scattered away from the direction of the incident beam are determined by a retardation potential method. Details of the design and construction of the apperatus are given elsewhere,[12] but a summarized description is given below.

VACUUM SYSTEMS

Fig. 1 shows a schematic diagram of the apparatus and its associated circuitry. The gun and collision chambers are represented respectively by the regions to the left and right of electrode E_5. Each of these chambers is separately pumped by a 300 l./sec oil diffusion pump. The gun and collision chamber pumps are backed respectively by a 33·4 l./min and a 140 l./min mechanical pump. Each of the diffusion pumps is separated from the corresponding chamber by a trap, which can hold about 3 l. of liquid nitrogen, and a 5·1 cm gate valve, which uses neoprene O-ring gaskets. The gas to be studied is admitted to the collision chamber through a set of high vacuum needle valves, which permit a fine adjustment of the pressure in that chamber. All electron scattering measurements are made under dynamic conditions, the gas flowing through the collision chamber. Since the two chambers are connected only by a 1·5 mm diam. pinhole, good differential pumping can be maintained. In general, the pressure within the gun chamber can be maintained at about 1/50 of that in the collision chamber when the pressure in the latter is of the order of 10^{-4} mm Hg. The pressures were read by calibrated ionization gauge tubes and circuits.

The electron gun and collision chambers are made of 6·03 cm ext. diam. brass tubes, with a wall thickness of 1·66 mm. They are closed at the ends by flanges made of non-magnetic stainless steel through which electrical leads pass via glass to metal seals. The two chambers are mechanically joined by a double flange of the same steel, on which electrode E_5 is mounted. This electrode is insulated from that flange by a flat quartz ring, represented in fig. 1 by the two hatched rectangles close to E_5. Electrode E_5 contains the pinhole which connects the two chambers. All gaskets in the chambers are of 0·76 mm diam. gold wire, and all materials used are resistant to temperatures of about 350°C. The two chambers can be baked at that temperature by an external oven which can be placed

around them. After baking the chambers for 24 h at about 300°C, with the pumps on and no gas flowing through the system, the pressure in each of them was usually about 3×10^{-7} mm Hg.

ELECTRON GUN

The electron gun consists of an oxide cathode heated by a tungsten filament and of five electrodes, represented by E_1 . . . E_5 in fig. 1. The oxide coating of the cathode has the shape of a circular disc with 3 mm diam. This cathode is usually operated at 1000°K. Electrode E_1, which is made of inconel, is mounted directly in front of the cathode and has a 5 mm diam. centre hole. It is usually operated at potentials 40-65 V positive with respect to the cathode. This results in a total emission of 3 to 5 mA.

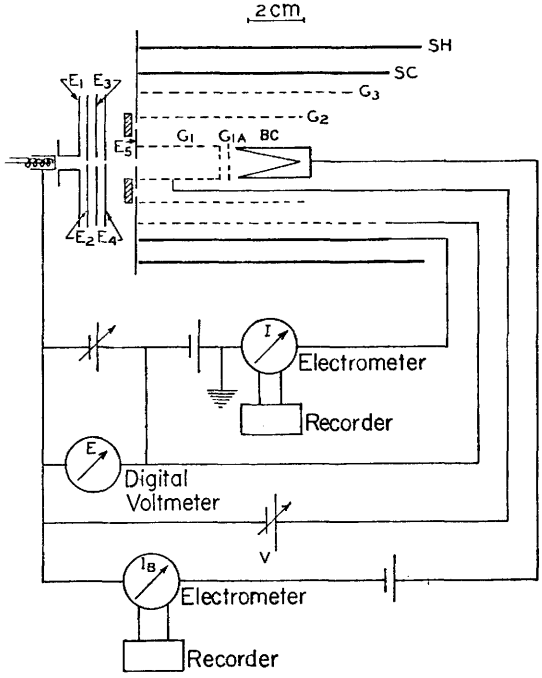

FIG. 1.—Schematic diagram of apparatus and circuitry.

Electrodes E_2, E_3 and E_4 are made of 0·80 mm thick inconel discs, 47·6 mm in diam. Their centre holes have diameters of 0·5, 1·0 and 0·5 mm respectively. The spacing between E_i and E_{i+1} ($i = 1, 2, 3$) is 1·5 mm. Electrodes E_2, E_3 and E_4 are usually operated as an Einzel lens with E_2 and E_4 equipotential and E_3 negative with respect to the other two. The voltage difference between E_5 and the cathode is positive and determines the energy with which the electron beam enters the collision chamber. Usually, E_2 and E_4 are operated at the same potential as E_5. The potential on E_3 is chosen so as to minimize the ratio of background current (current reaching collector SC) to beam current within the collision chamber.

Electrode E_5 is 5·7 mm away from E_4 and is made of a 0·25 mm thick gold disc mounted by means of an epoxy resin to a 2·5 cm diam. quartz disc, 1·6 mm thick, which contains a 12·5 mm hole in its centre. The electron beam passes from the gun chamber into the scattering chamber through the 1·5 mm diam. pinhole on E_5.

COLLISION CHAMBER

In the collision chamber there are several grids and collectors. First, there is the grid G_1. It s a cylinder made of tantalum gauze woven from 0·076 mm diam. wires with 19·7

wires/cm. This furnishes a transparency of 72 %. The diameter of G_1 is 12·5 mm and its length 25 mm. The end of G_1 away from E_5 is closed by a piece of tungsten gauze of 92 % transparency containing 39·4 wires/cm. Grid G_1 is operated at the same potential as E_5. Therefore, the space enclosed by G_1 and E_5 is free of electric fields. It is also made free of about 90 % of the earth's magnetic field by the use of two pairs of Helmholtz coils. The collisions between electrons and molecules take place in this region.

Four mm beyond the termination of G_1 there is another grid G_{1A} also made of the 92 % transparency tungsten. This grid serves a dual purpose. First, during the operation of the spectrometer, it is set at the same potential as G_1, whereas the beam collector BC which follows it is set at a higher potential. Grid G_{1A} thus prevents electric field penetration into the field-free region enclosed by G_1 and E_5. Secondly, it may be used to energy-analyze the electron beam.

After G_{1A} there is a beam collector BC, made of brass and shaped internally as a conical Faraday cage to provide multiple internal reflections of the incident electrons in order to decrease the background current. To decrease further the chance of reflection of electrons back into the collision chamber, a holding voltage of 50 V is applied between BC and G_{1A}. This voltage was crucial in order that a sufficiently low background current be reached.

Surrounding G_1 is another cylindrical grid G_2. It is made of the same tantalum gauze as G_1. Its diameter is 30 mm and its length 57 mm. Its purpose is to repel any positive ions which are formed by ionizing collisions between the electrons and the molecules under study. To this end it is placed at a potential 10 V positive with respect to G_1. Since positive ions would be formed with low kinetic energy, the repelling field thus produced is sufficient to prevent these positive ions from reaching the scattered electron collector SC.

Around G_2 there is a third cylindrical grid G_3 also made of the same tantalum gauze as G_1 and G_2. Its diameter is 45 mm and its length 71 mm. At the beginning of an experiment it is placed at a potential negative with respect to the cathode so that none of the scattered electrons has sufficient energy to pass through it and reach SC. The potential difference between G_3 and the cathode is then gradually increased. This decreases the repelling field between G_2 and G_3 which scattered electrons have to overcome to reach SC. Eventually elastically scattered electrons can overcome this field and reach SC, which produces a sudden rise in the current I to that collector. As the repelling field is further decreased, electrons having lost energy to the molecules being studied can now reach SC with additional sudden rises in the current to this collector. If at a potential difference of $|E|$ volts between G_3 and the cathode there is a sudden rise in I (as determined by a maximum in the derivative $dI/d|E|$ against $|E|$ curve), this corresponds to a molecular transition energy of $E = |E|$ eV after corrections for background and contact potential are made.

Surrounding G_3 is the scattered electron collector SC. It is made of tantalum foil 0·025 mm thick. Its diameter is 54 mm and its length 83 mm. It is surrounded by a shield SH of the same material whose diameter and length are 73 mm and 95 mm respectively. A constant holding potential of 40 to 50 V is applied between G_3 and SC to avoid electron reflection or secondary electron emission from SC.

All grids and collectors in the collision chamber are covered with a coating of platinum black formed by electrodeposition. Its purpose is to minimize the reflection of electrons off these surfaces.

ELECTRICAL CIRCUITS

Part of the circuitry employed is indicated in fig. 1. The potentials on electrodes E_2, E_3, E_4 and E_5, on grids G_1 and G_{1A} and G_2, on the shield and on the beam collector are applied relative to the cathode by circuits consisting each of two 90 V dry cells connected across a 300 kΩ, ten turn, helical resistor. A switching arrangement allows any of these circuits to be connected to an electrometer, which is provided with 8 linear current ranges from 1×10^{-3} through 1×10^{-11} A full-scale deflection. The response time of the electrometer can be varied from 0·1 to 30 sec. This electrometer is floating at the cathode potential, and its output is connected to a strip chart recorder. The beam current I_B reaching the beam collector is continuously recorded. The potential on E_1, relative to the cathode, is

applied by a regulated power supply having a voltage stability of 0·1 % and a ripple of less than 3 mV r.m.s. The use of a power supply on this electrode is convenient since the currents reaching E_1 are of the order of mA and would cause a rapid decay of dry cells. The variable potential on G_3 relative to the cathode is applied by a high-stability power supply having a drift of 0·01 %/h and a ripple of 500 μV r.m.s. or less. The potential between SC and G_3 is applied by the same type of circuit as that between G_1 and the cathode. The power to the cathode heater is obtained from a 110 V d.c. generator and a 720 Ω resistor in series with it.

The current I reaching SC is measured with a vibrating reed electrometer, which permits current readings by meter deflection down to 10^{-14} A full-scale. It is connected to a strip chart recorder on which I is registered as a function of E. All potentials are measured by an accurate digital voltmeter capable of measuring d.c. potential differences between 0·1 and 500 V to within 0·05 %.

GENERAL BEHAVIOUR OF THE APPARATUS

By adjustment of the several potentials it was possible to obtain a scattered current to beam current ratio, I/I_B, in the absence of gas in the collision chamber, ranging from about 4×10^{-2} at beam energies of 30 eV down to $1{\cdot}6\times10^{-4}$ at beam energies of 75 eV for $E = 13$ eV. The beam current was about 4×10^{-7} A in this range. These ratios were sufficiently small for the increase in I produced by the introduction of about 10^{-4} mm Hg of gas into the collision chamber to be adequate for gathering spectra. These ratios were achieved with the help of a one-quarter gauss axial magnetic field from a small horseshoe permanent magnet placed outside the gun chamber so as to minimize I/I_B in the absence of gas. At beam energies below 25 eV this ratio became too high to permit impact spectra to be obtained.

With about 10^{-4} mm Hg of test gas in the collision chamber, the variation of I with the holding voltage between G_3 and SC showed a plateau for values of 40 V and above. All spectral measurements were made in this plateau region. Also, the variation of I with the positive ion repelling field between G_2 and G_1 was determined and showed a plateau when G_2 was made 6 V or more positive with respect to G_1. Spectra were usually obtained with this potential difference equal to 10 V.

The current I due to gas phase scattering (the difference in the value of I with gas present and absent from the collision chamber, all other conditions being the same) was proportional to the beam current I_B and to the gas pressure p in the collision chamber, up to pressures of about 1 μ Hg. Above this pressure, the curve of I against p showed a downward curvature, as expected from the onset of double scattering. All spectra were gathered in the range for which the gas phase signal was proportional to both pressure and beam current, which satisfies the conditions for observing only single scattering events.

The procedure followed in obtaining the excitation spectra was the following. After the instrument was baked out and pumped down, a background curve of I against E was obtained with no gas in the collisional chamber. Curve B of fig. 2 represents a portion of one such curve. Then, the gas was admitted to the collision chamber through the needle valves of the inlet system. The flow rate was regulated to produce a steady-state pressure in that chamber in the proportionality region discussed above. This pressure was usually around 5×10^{-4} mm Hg. Then another curve of I against E was taken. The beam current I_B was simultaneously measured and adjusted to its initial value when necessary, which was very seldom. Curve A of fig. 2 represents a portion of such a curve for helium. Then, the background was subtracted to give the part of I due to gas-phase scattering and a smooth curve drawn through these difference points. In fig. 2 this is represented by curve C, which shows the sudden rises mentioned previously. Then, closely and equally spaced ordinates were read off this curve and used as input data for a digital computer programme which computed its derivative numerically using a sixth degree polynomial fitted to seven successive points of the curve. The derivative curve was then plotted. The one corresponding to fig. 2 is given in fig. 3. The vertical line in the left-hand side corner of this figure, and in all other excitation spectra figures reported here, represents the scatter in the derivative produced by the scatter in the reading of the ordinates from the smoothed

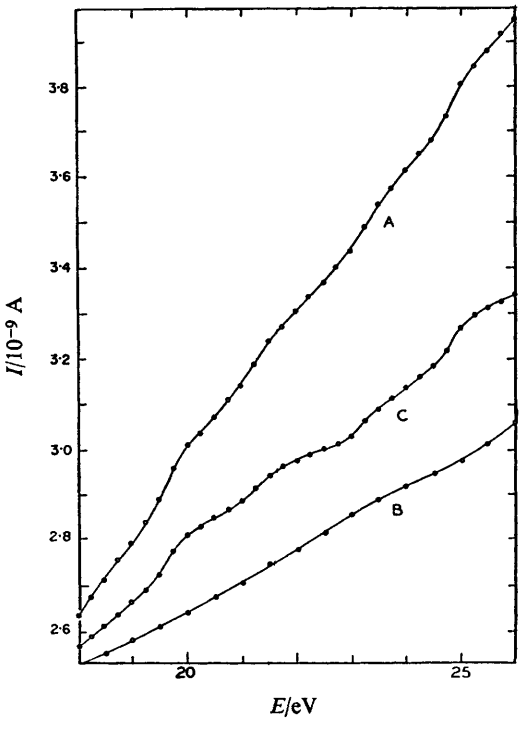

FIG. 2.—Variation of scattered electron current I with energy loss E for helium. Curve A: gas phase signal plus background; curve B: background, shifted upwards by $1{\cdot}64\times10^{-9}$ A; curve C: gas phase signal only, shifted upwards by $0{\cdot}81\times10^{-9}$ A. Incident electron beam energy, 50 eV; ion gauge reading, $5{\cdot}9\times10^{-4}$ mm Hg; $I_B = 4{\cdot}0\times10^{-7}$ A.

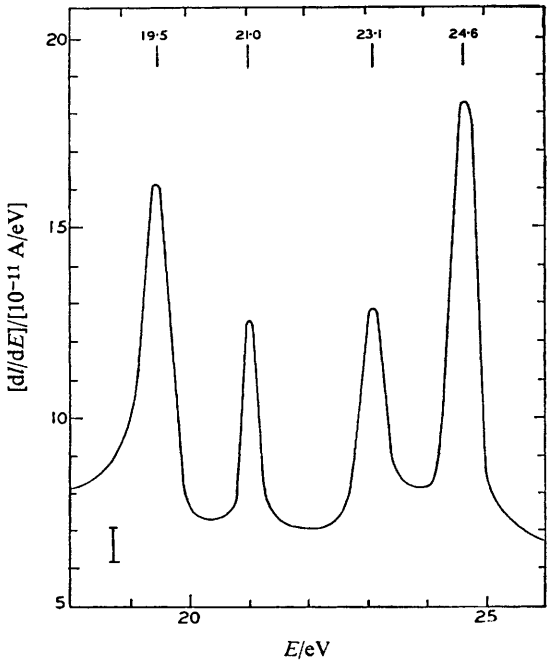

FIG. 3.—Excitation spectrum of helium; same conditions as for fig. 2.

difference curves of type B. It thus represents a lower limit to the error in the ordinates in those spectra. The horizontal scale of the derivative curve was then displaced to make the observed ionization energy fit the known value from optical or mass spectrometric experiments. No such correction was necessary for fig. 3. Usually this contact potential energy correction was 0·1-0·2 eV. This value is surprisingly low and probably attributable to the use of tantalum in the collision chamber grids and collectors.

EXCITATION SPECTRA OF HELIUM, ARGON AND HYDROGEN

Electron impact spectra for helium were obtained using a research grade quality of this gas furnished by the Linde Company and reported to be 99·99 % pure. It was used without further purification. Fig. 3 shows a spectrum for energy losses between 18 and 26 eV obtained using a beam energy of 50 eV and a gas pressure corresponding to an ion gauge reading of $5{\cdot}9 \times 10^{-4}$ mm Hg. Fig. 4 shows a similar spectrum for a 25 eV electron beam and an ion gauge reading of $2{\cdot}7 \times 10^{-4}$ mm Hg.

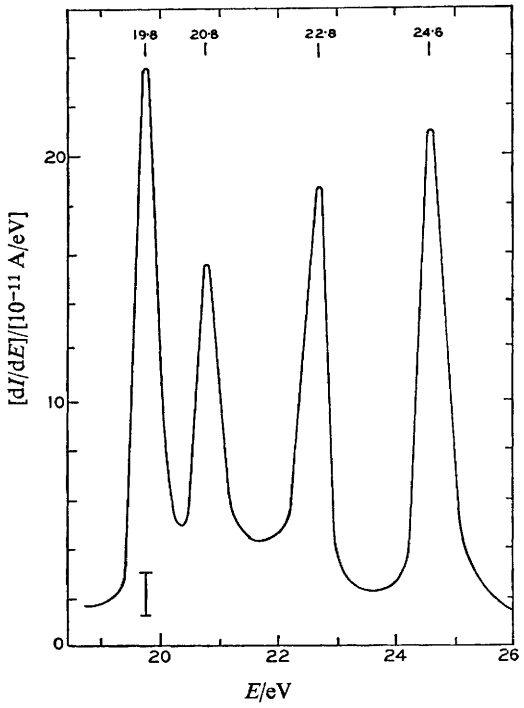

FIG. 4.—Excitation spectrum of helium; incident electron beam energy, 25 eV; ion gauge reading, $2{\cdot}7 \times 10^{-4}$ mm Hg; $I_B = 1{\cdot}0 \times 10^{-7}$ A.

The numbers at the top of those figures are the energies at which the maxima in the spectra were observed. The lowest electronic transition energies for helium,[13] from the ground 1^1S state, are 19·82 eV (2^3S), 20·61 eV (2^1S), 20·96 eV (2^3P), 21·22 eV (2^1P), 22·92 eV (3^1S) and 23·08 eV (3^1P). Higher energy states are so close together that they show up as a continuum between 22·8 eV and 24·6 eV in fig. 4. This is due to impact spectrum line broadening produced by the thermal energy spread of the incident electron beam and the fact that electrons scattered with the same energy in directions forming different angles with the undeflected electron beam have different components of the energy in the direction of the retardation field

between G_2 and G_3 which is essentially perpendicular to the incident beam. The optical ionization potential of helium [13] is 24·58 eV, whereas the values obtained from fig. 3 and 4 before correcting for contact potential, are 24·6 eV and 24·4 eV, respectively. Comparison of the transition energies obtained from fig. 3 and 4 with each other and with the optical values indicates that the resolution and accuracy of the instrument are about $\frac{1}{2}$ eV and $\pm \frac{1}{3}$ eV, respectively. The resolution is consistent with a thermal spread of 0·3 eV expected [14] from an oxide-coated cathode operated at about 1000°K. The estimated accuracy is consistent with almost all transition energies reported in this paper. The transitions to the 2^1S (20·61 eV), 2^1P (20·96 eV) and 2^1P (21·22 eV) states show up in our impact spectra as a single line peaking at 21·0 eV in fig. 3 and 20·8 eV in fig. 4, in excellent agreement with the optical data within the estimated accuracy and resolution.

In both helium spectra, the transition to the 2^3S state, although spin-forbidden in optical spectra, is very strong. This contrasts sharply with the spectra obtained by Lassettre,[7] using incident electron energies between 400 eV and 600 eV, who did not observe this transition. The reason for this behaviour is that at these high energies the Born approximation is valid and it furnishes spin-multiplicity selection rules identical to those of optical transitions. However, at the lower energies we employed (25 eV and 50 eV), exchange scattering [15] can occur and singlet to triplet transitions are permitted.

The ordinates in our impact spectra are roughly proportional (over a certain range of scattering angles) to a partially integrated differential collision cross-section. The ratio of the peak heights of two transitions should be, qualitatively, approximately equal to the ratio of the total collision cross-sections for these transitions. In spite of the very approximate nature of this equality and of the relatively large error in the ordinates of our spectra, it seems significant that in going from an incident beam energy of 25 eV (fig. 4) to one of 50 eV (fig. 3) the ratio of the intensities of the 19·8 and 23 eV transitions changes very little. The calculations of Bates *et al.*[16, 17] would have predicted a sharp decrease in this ratio. In any case, the empirical observation is that the $1^2S \rightarrow 2^3S$ spin-forbidden transition can be easily detected in our instrument even when the incident electron beam energy is 30 eV above the excitation energy.

Spectra for argon were obtained using research grade quality gas furnished by the Linde Company and reported to be 99·995 % pure. This gas was used without further purification. One of the argon spectra obtained with a 50 eV electron beam is given in fig. 5. The lowest excited states of argon[13] are a triplet and a singlet which are at 11·6 eV and 11·8 eV respectively above the ground state. The measured peak at 12·2 eV is not in good agreement with these values. In other argon impact spectra the measured value was 11·9 eV, in better agreement. The next set of argon levels lies between 12·9 and 13·25 eV, with which the second peak of fig. 5, at 12·9 eV, agrees. Finally, the rest of the argon levels, up to ionization, are too close together to be resolved in our instrument.

It is seen from fig. 5 that the peak corresponding to elastic scattering has a maximum at about 2·2 eV rather than at 0 eV. This type of shift was observed in every impact spectrum obtained with our apparatus. At first, it might seem due to contact potentials. However, the contact potential correction to the energy scale determined by the ionization potential was usually never more than about 0·2 eV and made all excitation energies agree well with the optical ones. Moreover, since the electron beam energy is not changed during the gathering of a spectrum (contrary to the determination of an ionization efficiency curve in mass spectrometry), variations in the incident beam energy are not the explanation. The cause of this elastic

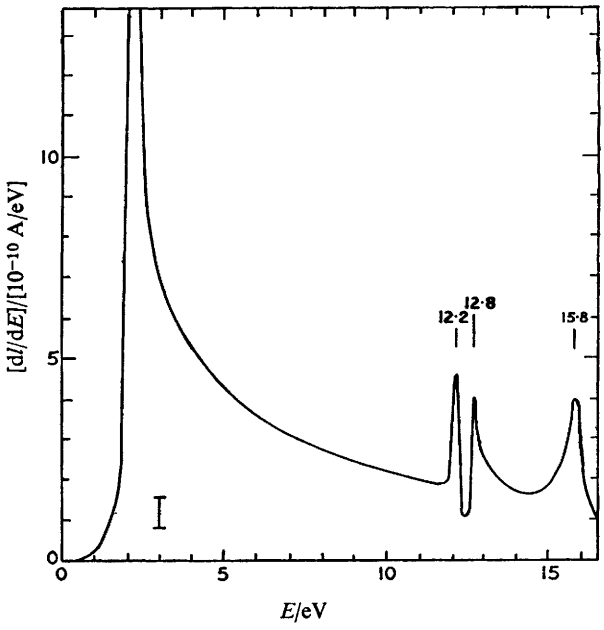

FIG. 5.—Excitation spectrum of argon; incident electron beam energy, 50 eV; ion gauge reading, $6{\cdot}4\times10^{-4}$ mm Hg; $I_B = 4{\cdot}7\times10^{-7}$ A.

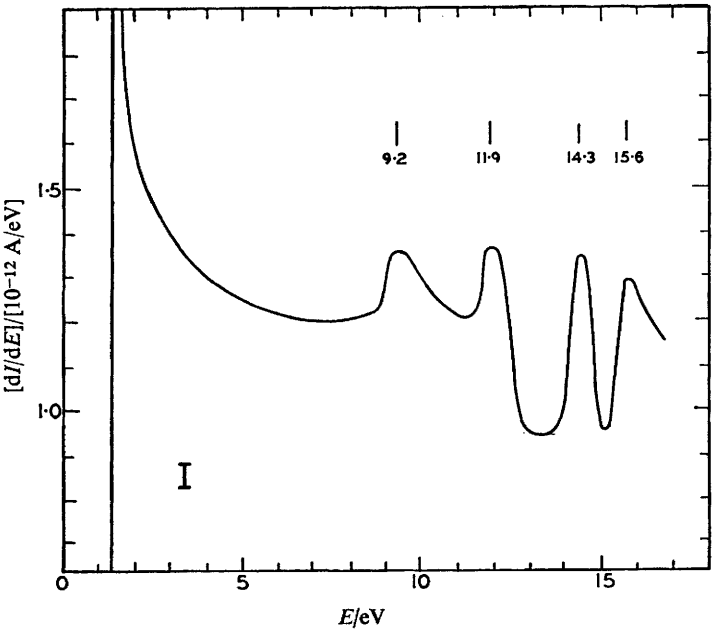

FIG. 6.—Excitation spectrum of molecular hydrogen; incident electron beam energy, 60 eV; ion gauge reading, 2×10^{-4} mm Hg; $I_B = 2{\cdot}3\times10^{-7}$ A.

peak shift is not clearly understood at present. However, the spectra obtained for helium, argon and hydrogen (see next paragraph) clearly show that only the elastic peak has this shift, and that the electronic excitation energies are not affected by its existence.

Research grade hydrogen, also supplied by the Linde Company and reported as being 99·9 % pure was used without further purification to obtain the impact spectrum of hydrogen given in fig. 6 for a 60 eV incident beam. The excitations are represented by bands which are much broader than in the rare-gas impact spectra.

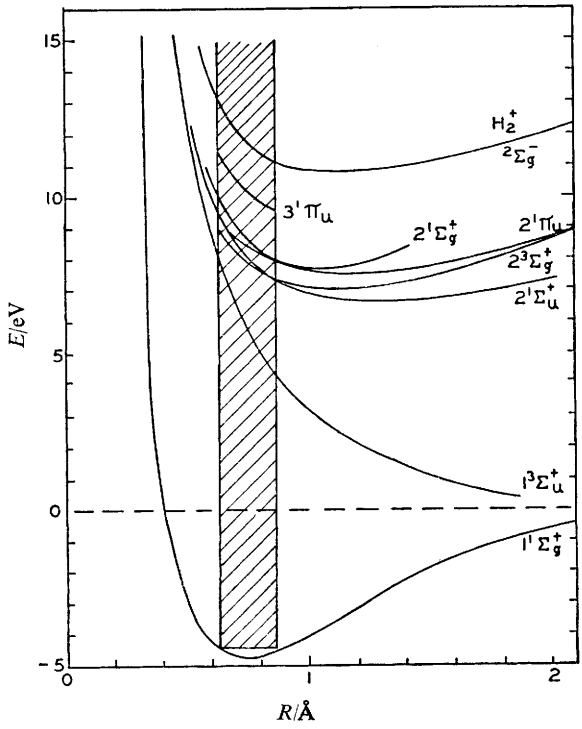

FIG. 7.—Potential energy curves for molecular hydrogen.

This is a consequence of the variation of electronic energy with internuclear distance and of the fact that in the range of electron energies used in these experiments the Franck-Condon principle is obeyed.[18] According to it, transitions from the ground state must occur vertically within the shaded area of fig. 7. This figure contains the potential energy curves for the ground state and several electronically excited states of molecular hydrogen.[18-20] The four bands observed in fig. 6 are in good agreement with those which one would predict *a priori* from fig. 7. The band whose maximum lies at 9·2 eV corresponds to the transition $1^1\sum_g^+ \rightarrow 1^3\sum_u^+$. Thus, a singlet to triplet molecular transition is clearly observed with a beam energy about 50 eV above the excitation energy.

EXCITATION SPECTRA OF ETHYLENE

The ethylene, furnished by The Matheson Company and reported as being 99·5 mole % pure, was used without further purification. Spectra were obtained at 40 eV, 50 eV, and 75 eV incident electron beam energies and are given in fig. 8, 9

and 10, respectively. The vacuum ultra-violet spectrum of ethylene shows an absorption maximum at 7·66 eV corresponding to the $V \leftarrow N$ band of the π-electron system,[21] onsets of 7·1 eV, 8·2 eV, 8·65 eV for three $R \leftarrow N$ Rydberg series,[22] and an ionization potential of 10·45 eV.[22] In fig. 8 and 9 the contact potential corrections were determined as usual from the ionization potential. The bands peaking at 7·7 and 8·8 eV are in good agreement with the optical values just mentioned. In fig. 10 the contact potential correction was determined from the $V \leftarrow N$ optical transition energy [21] because the ionization potential in this particular spectrum seemed to be in large error. In all these three figures the elastic peak occurs at 2·1 eV.

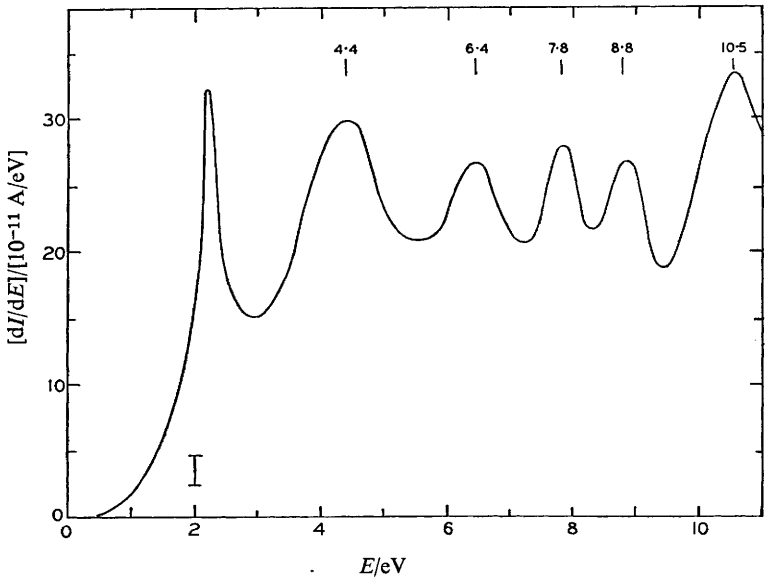

FIG. 8.—Excitation spectrum of ethylene; incident electron beam energy, 40 eV° ions gauge reading, 2×10^{-4} mm Hg; $I_B = 1{\cdot}6 \times 10^{-7}$ A.

From fig. 8 and 9 a low-lying transition energy with an average value of 4·6 eV is obtained. This is in good agreement with the optically forbidden value of 4·6 eV obtained by Evans in optical absorption spectra using the oxygen-intensification technique [23] and assigned to a vertical $T \leftarrow N$ transition of the π electron system.[23, 24] The peak at about 6·5 eV in fig. 8, 9 and 10, is in good agreement with an optically forbidden transition energy of 6·4 eV obtained indirectly by Potts.[25] He measured forbidden band transition energies in optical absorption spectra of several methylethylenes, cyclohexene, and 1-hexene, taken at room temperature and at liquid-nitrogen temperature. He had assigned this energy to the $T \leftarrow N$ transition, but after Evans' experiments it was tentatively re-assigned by Mulliken [24] to a Rydberg triplet state.

Comparison of the 4·6 eV peak intensities with the 7·7 eV ones in fig. 8-10 shows that it decreases with increasing incident beam energy, becoming a shoulder in the elastic peak when this energy reaches 75 eV. This is expected for spin-forbidden transitions [2] and is consistent with Evans' assignment. A similar comparison between the 6·5 eV and 7·7 eV peak intensities shows that their ratio does not decrease to any significant extent in the 40 eV to 75 eV range of incident electron energies used, suggesting that the 6·5 peak, although optically forbidden, does not correspond

to a singlet-triplet transition.[2] Recently, Berry [26] has ascribed it to a transition analogous to the $n \rightarrow \pi^*$ one of formaldehyde.[27] Such assignment would be consistent with the intensity dependence described above.

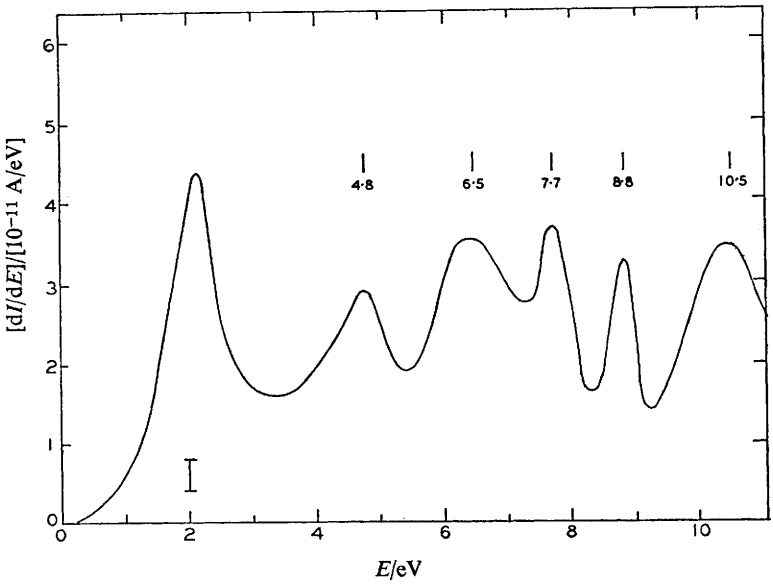

FIG. 9.—Excitation spectrum of ethylene; incident electron beam energy, 50 eV; ion gauge reading, $3{\cdot}8 \times 10^{-4}$ mm Hg; $I_B = 2{\cdot}6 \times 10^{-7}$ amp.

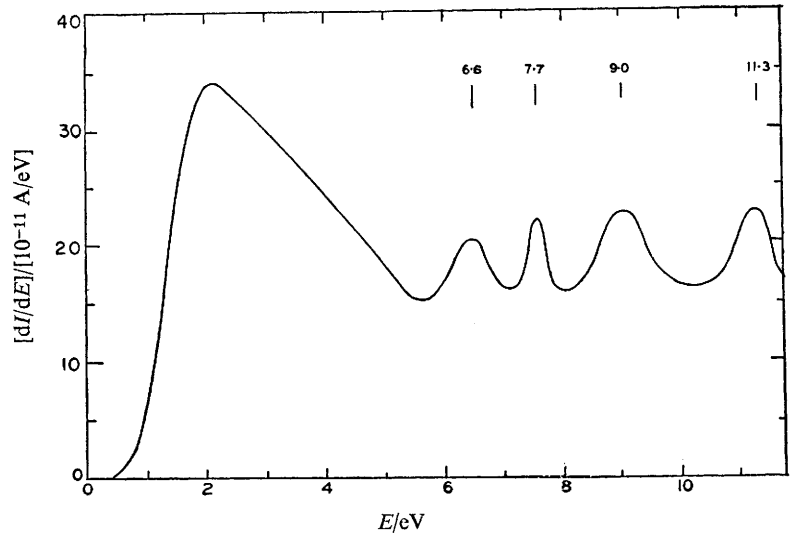

FIG. 10.—Excitation spectrum of ethylene; incident electron beam energy, 75 eV; ion gauge reading, $2{\cdot}9 \times 10^{-4}$ mm Hg; $I_B = 3 \times 10^{-7}$ A.

In the electron-trap method used by Schulz [9] for observing electronic excitation energies in atoms and molecules, all excitations are determined with electrons whose energies are slightly (usually 0·3 eV) above the excitation energies. Therefore,

this otherwise excellent method does not permit one to obtain the additional information which results from observing the variation of peak intensities with incident electron beam energy over a wide range of the latter.

CONCLUSIONS

Our results indicate that low-energy electron-impact spectroscopy can be a very useful tool to help elucidate the electronic structure of molecules, specially their low-lying optically-forbidden electronic states. Not only can such states be easily located, but it seems to be possible to distinguish between spin-forbidden and symmetry-forbidden transitions by observing the variation of peak intensities with incident electron beam energy. Improvement in accuracy and resolution can be expected. Since the spectrometer can be operated at 350°C, and since a vapour pressure of 10^{-4} mm Hg is sufficient for an impact spectrum to be obtained, a large number of molecules can be studied by this technique.

The authors wish to thank Dr. Siao-fang Sun for his participation in the early stages of the development of the spectrometer here reported.

[1] Franck and Hertz, *Verh. dtsh. physik. Ges.*, 1914, **16,** 457; *Physik. Z.*, 1916, **17,** 409.
[2] Massey and Burhop, *Electronic and Ionic Impact Phenomena* (Oxford University Press, London, 1952), pp. 141-146.
[3] Jones and Whiddington, *Phil. Mag.*, 1928, **6,** 889.
[4] Glockler and Wilson, *J. Amer. Chem. Soc.*, 1932, **54,** 4544.
[5] Rudberg, *Proc. Roy. Soc. A*, 1930, **129,** 629.
[6] Rudberg, *Proc. Roy. Soc. A*, 1931, **130,** 182.
[7] Lassettre, *Radiation Res.*, 1959, suppl., **1,** 530, and a series of *Ph.D. Diss.* and of U.S. Air Force reports mentioned in this reference.
[8] ref. (2), pp. 137-139.
[9] Schulz, *Physic. Rev.*, 1958, **112,** 150; *J. Chem. Physics*, 1960, **33,** 1661.
[10] Kuppermann and Raff, *J. Chem. Physics*, 1962, **37,** 2497.
[11] Arnot and Baines, *Proc. Roy. Soc. A*, 1935, **151,** 256.
[12] Raff, L. M., *Ph.D. Thesis* (University of Illinois, Urbana, 1962).
[13] Moore, *Atomic Energy Levels* (Nat. Bur. Stand. circ. 467, 1949), vol. I.
[14] Spangenberg, *Vacuum Tubes* (McGraw-Hill, New York, 1948), pp. 25-26.
[15] Oppenheimer, *Physic. Rev.*, 1928, **32,** 361.
[16] Bates, Fundaminsky, Leech and Massey, *Phil. Trans. A*, 1950, **243,** 117.
[17] ref. (2), pp. 159-60.
[18] ref. (2), pp. 221, 230.
[19] Kolos and Roothaan, *Rev. Mod. Physics*, 1960, **32,** 219.
[20] Tanaka, *Sci. Papers Inst. Physic. Chem. Res. Tokyo*, 1944, **42,** 49.
[21] Wilkinson and Mulliken, *J. Chem. Physics*, 1955, **23,** 1895.
[22] Price and Tutte, *Proc. Roy. Soc. A*, 1940, **174,** 207.
[23] Evans, *J. Chem. Soc.*, 1960, 1735.
[24] Mulliken, *J. Chem. Physics*, 1960, **33,** 1596.
[25] Potts, *J. Chem. Physics*, 1955, **23,** 65.
[26] Berry, *J. Chem. Physics*, 1963, **38,** 1934.
[27] Mason, *Mol. Physics*, 1962, **5,** 343.